cells

MDPI

Article

Pharmacological Inhibition of Wee1 Kinase Selectively Modulates the Voltage-Gated Na^+ Channel 1.2 Macromolecular Complex

Nolan M. Dvorak †, Cynthia M. Tapia †, Timothy J. Baumgartner, Jully Singh, Fernanda Laezza and Aditya K. Singh *

Department of Pharmacology and Toxicology, University of Texas Medical Branch, Galveston, TX 75901, USA; nmdvorak@utmb.edu (N.M.D.); cmtapia@utmb.edu (C.M.T.); tjbaumga@utmb.edu (T.J.B.); jusingh@utmb.edu (J.S.); felaezza@utmb.edu (F.L.)

* Correspondence: adsingh@utmb.edu; Tel.: +1-409-772-9759

† These authors contributed equally to this work.

Abstract: Voltage-gated Na^+ (Na_V) channels are a primary molecular determinant of the action potential (AP). Despite the canonical role of the pore-forming α subunit in conferring this function, protein–protein interactions (PPI) between the Na_V channel α subunit and its auxiliary proteins are necessary to reconstitute the full physiological activity of the channel and to fine-tune neuronal excitability. In the brain, the Na_V channel isoforms 1.2 ($Na_V1.2$) and 1.6 ($Na_V1.6$) are enriched, and their activities are differentially regulated by the Na_V channel auxiliary protein fibroblast growth factor 14 (FGF14). Despite the known regulation of neuronal Na_V channel activity by FGF14, less is known about cellular signaling molecules that might modulate these regulatory effects of FGF14. To that end, and building upon our previous investigations suggesting that neuronal Na_V channel activity is regulated by a kinase network involving GSK3, AKT, and Wee1, we interrogate in our current investigation how pharmacological inhibition of Wee1 kinase, a serine/threonine and tyrosine kinase that is a crucial component of the G2-M cell cycle checkpoint, affects the $Na_V1.2$ and $Na_V1.6$ channel macromolecular complexes. Our results show that the highly selective inhibitor of Wee1 kinase, called Wee1 inhibitor II, modulates FGF14:$Na_V1.2$ complex assembly, but does not significantly affect FGF14:$Na_V1.6$ complex assembly. These results are functionally recapitulated, as Wee1 inhibitor II entirely alters FGF14-mediated regulation of the $Na_V1.2$ channel, but displays no effects on the $Na_V1.6$ channel. At the molecular level, these effects of Wee1 inhibitor II on FGF14:$Na_V1.2$ complex assembly and FGF14-mediated regulation of $Na_V1.2$-mediated Na+ currents are shown to be dependent upon the presence of Y158 of FGF14, a residue known to be a prominent site for phosphorylation-mediated regulation of the protein. Overall, our data suggest that pharmacological inhibition of Wee1 confers selective modulatory effects on $Na_V1.2$ channel activity, which has important implications for unraveling cellular signaling pathways that fine-tune neuronal excitability.

Keywords: voltage-gated Na^+ (Na_V) channels; fibroblast growth factor 14 (FGF14); Wee1 kinase; patch-clamp electrophysiology

Citation: Dvorak, N.M.; Tapia, C.M.; Baumgartner, T.J.; Singh, J.; Laezza, F.; Singh, A.K. Pharmacological Inhibition of Wee1 Kinase Selectively Modulates the Voltage-Gated Na^+ Channel 1.2 Macromolecular Complex. *Cells* **2021**, *10*, 3103. https://doi.org/10.3390/cells10113103

Academic Editor: T.K.S. Kumar

Received: 2 October 2021
Accepted: 8 November 2021
Published: 10 November 2021

1. Introduction

The activity of voltage-gated Na^+ (Na_V) channels is the primary determinant of the initiation and propagation of action potentials (AP) in excitable cells [1]. Structurally, the pore-forming α subunit of Na_V channels, of which nine different isoforms have been described ($Na_V1.1$–$Na_V1.9$) [1], is comprised of four transmembrane domains (DI-DIV), and each transmembrane domain is comprised of six segments (S1–S6) [2,3]. Despite the central role of this pore-forming α subunit in conferring Na_V channel activity, the full physiological function of the Na_V channel is dependent upon protein–protein interactions (PPIs) between the Na_V channel α subunit and its auxiliary proteins [4,5]. Among these auxiliary proteins,

intracellular fibroblast growth factors (iFGF; FGF11–FGF14) represent an important family of accessory proteins that regulate the kinetics and trafficking of Na_v channels through direct PPIs with the C-terminal domains (CTD) of different Na_v channel isoforms [6–10].

In the central nervous system (CNS), FGF14 is a particularly prominent Na_v channel auxiliary protein that regulates resurgent sodium current (I_{NaR}) [11,12] and differentially modulates transient sodium currents (I_{Na}) mediated by $Na_v1.2$ versus $Na_v1.6$ channels [7]. Despite these regulatory effects of FGF14 on different types of neuronal Na+ currents and differential regulation of CNS Na_v channel isoforms, less is known about cellular signaling molecules that might modulate FGF14′s effects on these biophysical processes.

To that end, we previously performed a high throughput screening of kinase inhibitors against different Na_v channel macromolecular complexes using an optimized in-cell assay to identify modulators of FGF14′s complex assembly with different Na_v channel isoforms [13–15]. Through these investigations, in tandem with orthogonal and functional validation modules, we have identified GSK3 [16], AKT [17], and JAK2 [14] as important kinases that regulate FGF14:$Na_v1.6$ complex assembly and $Na_v1.6$ channel activity; although, the regulatory effects of these kinases on other iFGF:Na_v complexes, such as FGF14:$Na_v1.2$, are less well characterized.

In addition to the established roles of the aforementioned kinases in regulating FGF14′s PPI with Na_v channel isoforms, our previous investigations have suggested a potential role of Wee1 kinase in regulating PPIs involved in Na_v channel macromolecular complex assembly [13,14,17]. Wee1 is a serine/threonine and tyrosine kinase with an established role in regulating the G2-M cell-cycle checkpoint in which the kinase negatively regulates entry of cells into mitosis to allow for DNA repair [18]; although, its effect on neuronal activity is less well-characterized. Providing some insights into the latter, it has been shown that pharmacological inhibition of Wee1 kinase through the employment of some Wee1 kinase inhibitors modulates the complex assembly of various iFGF:Na_v channel pairs [13,14]. Additionally, Wee1 kinase activity has been shown to be modulated by GSK3 [19–21] and to potentially increase AKT activity [22], which could have important implications for conferring indirect effects on Na_v channel activity given the known regulatory effects of these kinases on Na_v channel kinetics and trafficking [13,14,16,17].

In the present investigation, we focus squarely on assessing this potential regulation of the Na_v channel conferred by Wee1 kinase. In particular, we focused on investigating the regulatory effects of Wee1 kinase on the FGF14:$Na_v1.2$ and FGF14:$Na_v1.6$ complexes on account of FGF14 previously having been shown to confer differential regulation of these two CNS Na_v channel isoforms [7]. To that end, we employ the selective inhibitor of Wee1 kinase, called Wee1 Inhibitor II, and show that pharmacological inhibition of Wee1 kinase confers marked modulatory effects on FGF14:$Na_v1.2$ complex assembly, but not FGF14:$Na_v1.6$ complex assembly. Functionally, these effects of Wee1 inhibitor II are recapitulated, as pharmacological inhibition of Wee1 kinase alters FGF14-mediated regulation of the $Na_v1.2$ channel, but not of the $Na_v1.6$ channel. At the molecular level, these effects of Wee1 inhibitor II on FGF14:$Na_v1.2$ complex assembly and the activity of the $Na_v1.2$ channel macromolecular complex are shown to be dependent upon the presence of a residue of FGF14 previously shown to be prominent site for phosphorylation-mediated regulation of the protein [14]. Overall, these findings suggest that Wee1 kinase selectively modulates FGF14-mediated regulation of the $Na_v1.2$ channel, which has important implications for understanding molecular mechanisms that fine-tune neuronal excitability.

2. Materials and Methods

2.1. Chemicals

D-luciferin (Gold Biotechnology, St. Louis, MO, USA) was prepared as a 30 mg/mL stock solution in phosphate-buffered saline (PBS), and stored at −20 °C. Wee1 inhibitor II (Calbiochem, San Diego, CA, USA) was reconstituted in 100% dimethyl sulfoxide (DMSO; Sigma-Aldrich, St. Louis, MO, USA) as 50 mM stock solutions and stored at −20 °C.

2.2. Plasmid Constructs

The following plasmid constructs used in this study were engineered and characterized as previously described [8,14,15,23–28]: CLuc-FGF14, CD4-$Na_v1.2$ CTD-NLuc, CD4-$Na_v1.6$ CTD-NLuc, GFP, FGF14-GFP, and $FGF14^{Y158A}$-GFP.

2.3. Cell Culture

HEK293 cells were cultured as previously described [26,29–31], with different concentrations of G418 (Invitrogen, Carlsbad, CA, USA) added to the media to ensure stable $Na_v1.2$ and $Na_v1.6$ expression.

2.4. Split-Luciferase Complementation Assay (LCA)

The split-lucifease complementation assay (LCA) was performed as previously described [15,23]. Briefy, HEK293 cells were transiently transfected with either the CLuc-FGF14 and CD4-$Na_v1.2$ CTD-NLuc or CLuc-FGF14 and CD4-$Na_v1.6$ CTD-NLuc pairs of DNA constructs using Lipofectamine 2000 (Invitrogen) according to the manufacturer's instructions. 48 h post-transfection, transiently transfected cells were replated into CELLSTAR μClear® 96-well tissue culture plates (Greiner Bio-One, Monroe, NC, USA). After 24 h, medium was replaced with serum-free, phenol-red free, 1:1 DMEM/F12 (Invitrogen) containing Wee1 inhibitor II (Calbiochem) dissolved in DMSO (1–150 μM) or DMSO alone. The final concentration of DMSO was maintained at 0.5% for all wells. Following 2 h incubation at 37 °C, the reporter reaction was initiated by addition of 100 μL substrate solution containing 1.5 mg/mL D-luciferin (Gold Biotechnologies) dissolved in PBS. Luminescence readings were then performed using a Synergy™ H1 Multi-Mode Microplate Reader (BioTek, Winooski, VT, USA). Acquired data was then analyzed as previously described [15,23].

2.5. Whole-Cell Voltage-Clamp Recordings in Heterologous Cells

HEK-$Na_v1.2$ or HEK-$Na_v1.6$ cells were transiently transfected with pQBI-GFP, pQBI-FGF14-GFP, or pQBI-FGF14Y158A-GFP constructs. Twenty-four hours post-transfection, transiently transfected cells were plated at low density onto glass cover slips. After at least 2 h incubation, cover slips were transferred to a recording chamber containing extracellular recording solution comprised of the following salts: 140 mM NaCl; 3 mM KCl; 1 mM $MgCl_2$; 1 mM $CaCl_2$; 10 mM HEPES; and 10 mM glucose (final pH = 7.3; all salts purchased from Sigma-Aldrich). For control recordings, DMSO was added to the extracellular solution, whereas for recordings to characterize the effects of Wee1 inhibitor II (Calbiochem), the compound was added to the extracellular solution. The concentration of DMSO was maintained at 0.1% in both conditions. Cover slips were incubated for 30 min in extracellular solution containing vehicle or Wee inhibitor II (Calbiochem) prior to the start of recordings. For these recordings, borosilicate glass pipettes (Harvard Apparatus, Holliston, MA, USA) with a resistance of 3–5 MΩ, which were manufactured using a PC-100 vertical Micropipette Puller (Narishige International Inc., East Meadow, NY, USA), were filled with an intracellular solution comprised of the following salts: 130 mM CH_3O_3SCs; 1 mM EGTA; 10 mM NaCl; and 10 mM HEPES (pH = 7.3; all salts purchased from Sigma-Aldrich). After GΩ seal formation and entry into the whole-cell configuration, four voltage-clamp protocols were employed. The current–voltage (IV) protocol entailed voltage-steps from −100 mV to +60 mV from a holding potential of −70 mV. The voltage-dependence of steady-state inactivation protocol entailed a paired-pulse protocol during which, from the holding potential, cells were stepped to varying test potentials between −120 mV and +20 mV prior to a test pulse to −20 mV. For long-term inactivation, the voltage-clamp protocol entailed four depolarizations at 0 mV for 16 ms separated by three recovery intervals at −90 mV for 40 ms. For use-dependency, cells were stimulated using a train of 20 depolarization steps to −10 mV at a frequency of 10 Hz [32]. Recordings were performed using either an Axopatch 200B or Multiclamp 700B amplifier (Molecular Devices, Sunnyvale, CA, USA). Membrane capacitance and series resistance were estimated

using the dial settings on the amplifier, and capacitive transients and series resistances were compensated by 70–80%. Data acquisition and filtering occurred at 20 and 5 kHz, respectively, before digitization and storage. Clampex 9.2 software (Molecular Devices) was used to set experimental parameters, and electrophysiological equipment was interfaced to this software using a Digidata 1200 analog–digital interface (Molecular Devices). Acquired data was then analyzed as previously described [27,28,30,31,33].

3. Results

3.1. Pharmacological Inhibition of Wee1 Kinase Modulates FGF14:Na$_v$1.2, but Not FGF14:Na$_v$1.6, Complex Assembly in a FGF14^{Y158}-Dependent Manner

To study the regulatory effects of Wee1 kinase on FGF14′s PPI with Na$_v$ channel isoforms, we employed the pharmacological inhibitor of Wee1 kinase called Wee1 inhibitor II (Calbiochem). Wee1 inhibitor II (chemical name: 6-Butyl-4-(2-chlorophenyl)-9-hydroxypyrrolo[3, 4-c] carbazole-1,3(2H,6H)-dione), also referred to as compound 103 when first described [34], inhibits Wee1 kinase activity with an IC$_{50}$ value of 59 nM [34]. Importantly, Wee1 inhibitor II displays ~590-fold selectivity over the related kinase Chk1, displaying an IC$_{50}$ value of 35 μM toward the respective kinase [34]. Among Wee1 kinase inhibitors disclosed, these two combined features of Wee1 inhibitor II (i.e., IC$_{50}$ values of 59 nM and 35 μM toward Wee1 and Chk1, respectively) conferred it with the best Chk1 IC$_{50}$ to Wee1 IC$_{50}$ ratio, marking it as currently the most targeted pharmacological inhibitor of Wee1 kinase activity [34].

Using an in-cell, split-luciferase complementation assay (LCA) previously optimized by our laboratory to identify modulators of the assembly of FGF:Na$_v$ channel pairs [15,23], we tested the effects of pharmacological inhibition of Wee1 kinase on FGF14:Na$_v$1.2 and FGF14:Na$_v$1.6 complex assembly. In our studies, HEK293 cells were transiently transfected with either the CD4-Na$_v$1.2 CTD-NLuc and CLuc-FGF14 cDNA constructs or the CD4-Na$_v$1.6 CTD-NLuc and CLuc-FGF14 cDNA constructs. Resultantly, when FGF14 interacts with the CTD of the Na$_v$1.2 or Na$_v$1.6 channel, there is reconstitution of the NLuc and CLuc fragments of the luciferase enzyme, which, in the presence of the substrate luciferin, gives rise to a robust luminescence signal.

When tested for its effects on FGF14:Na$_v$1.2 complex assembly, Wee1 inhibitor II gave rise to a dose-dependent decrease in FGF14:Na$_v$1.2 complex assembly, as evidenced by the reduction in the luminescent signal observed in the presence of concentrations of Wee1 inhibitor II greater than or equal to 15 μM (Figure 1A). Plotting percentage luminescence as a function of the log concentration of Wee1 inhibitor II, the IC$_{50}$ value of the pharmacological inhibitor of Wee1 kinase as it relates to decreasing FGF14:Na$_v$1.2 complex assembly was determined to be 16.51 μM (Figure 1A).

Based upon the Y158 residue of FGF14 (FGF14^{Y158}) serving as a prominent site for phosphorylation-mediated regulation of the protein [14], we next investigated if Wee1 kinase might exert its regulatory effects on FGF14:Na$_v$1.2 complex assembly through a mechanism dependent upon the presence of the residue. When tested for its effects on FGF14:Na$_v$1.2 complex assembly in conditions in which FGF14^{WT} was mutated to FGF14^{Y158A}, Wee1 inhibitor II, even at the highest concentration tested (i.e., 150 μM), failed to reduce the luminescent signal by greater than 20% compared to per plate control wells treated with 0.5% DMSO (Figure 1B). These findings, in stark contrast to those observed in the WT condition where high concentrations of Wee1 inhibitor II conferred changes in the luminescent signal of greater than or equal to 80% (Figure 1A), provide strong evidence that the mechanism of action of pharmacological inhibition of Wee1 kinase as it relates to regulating FGF14:Na$_v$1.2 complex assembly is dependent upon the presence of FGF14^{Y158}.

Given that FGF14 confers differential regulation of the Na$_v$1.2 and Na$_v$1.6 channels [7], we next investigated if there were potentially different effects of pharmacological inhibition of Wee1 kinase on FGF14:Na$_v$1.2 versus FGF14:Na$_v$1.6 complex assembly. In stark contrast to the robust modulatory effects on FGF14:Na$_v$1.2 complex assembly conferred by Wee1 inhibitor II, pharmacological inhibition of Wee1 kinase exerted no noticeable effects on

FGF14:$Na_v1.6$ complex assembly (Figure 1C). Overall, these data suggest that Wee1 kinase might exert selective regulation of the $Na_v1.2$ channel macromolecular complex.

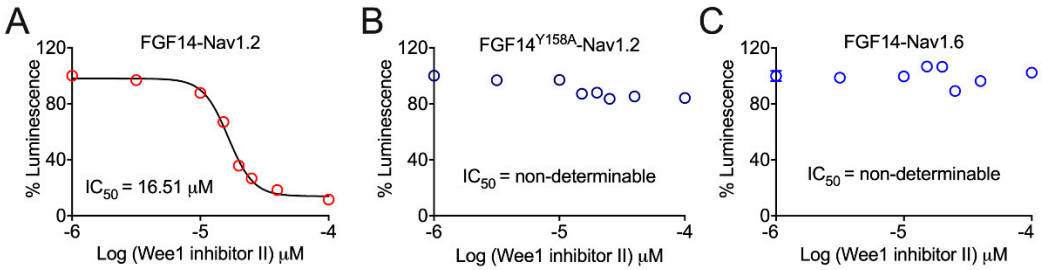

Figure 1. Evaluation of the effects of Wee1 inhibitor II on FGF14:$Na_v1.2$ and FGF14:$Na_v1.6$ complex assembly. (**A**) Percentage luminescence (normalized to per plate control wells treated with 0.5% DMSO; n = 32 wells per plate) plotted as a function of log concentration of Wee1 inhibitor II to characterize dose-dependent effects of pharmacological inhibition of Wee1 kinase on FGF14:$Na_v1.2$ complex assembly (range of concentrations tested = 1 μM–150 μm; n = 6 wells per concentration). (**B**) Effects of different concentrations (range = 1 μM–150 μM; n = 6 wells per concentration) of Wee1 inhibitor II on $FGF14^{Y158A}$:$Na_v1.2$ complex assembly. (**C**) Effects of different concentrations of Wee1 inhibitor II (range = 1 μM–150 μM; n = 6 wells per concentration) on FGF14:$Na_v1.6$ complex assembly. Data are represented as mean ± SEM.

3.2. Pharmacological Inhibition of Wee1 Kinase Modulates FGF14-Mediated Regulation of $Na_v1.2$ Channels

Having shown that pharmacological inhibition of Wee1 kinase confers modulatory effects on FGF14:$Na_v1.2$ complex assembly (Figure 1A), we next sought to investigate if these alterations in complex assembly resulted in changes in the function of the $Na_v1.2$ channel. To do so, HEK293 cells stably expressing the $Na_v1.2$ channel (HEK-$Na_v1.2$) [26,29,30] were transiently transfected with either GFP (HEK-$Na_v1.2$-GFP) or FGF14-GFP (HEK-$Na_v1.2$-FGF14-GFP). Cells were then incubated for 30 min with either vehicle (0.1% DMSO) or 15 μM of Wee1 inhibitor II, a concentration selected on the basis of it being close to the IC_{50} value of the compound as determined in the LCA (Figure 1A). After incubation, whole-cell voltage-clamp recordings were performed to characterize the effects of pharmacological inhibition of Wee1 kinase on the activity of $Na_v1.2$ channels (Figure 2; Tables 1 and 2).

Consistent with previous investigations [7], co-expression of FGF14-1b, the isoform of FGF14 studied in this investigation, with the $Na_v1.2$ channel α subunit in heterologous leads to a reduction in $Na_v1.2$-mediated peak I_{Na} density (−128.7 ± 5.7 pA/pF (n = 11) and −89.24 ± 7.7 pA/pF (n = 11) for HEK-$Na_v1.2$-GFP + DMSO and HEK-$Na_v1.2$-FGF14-GFP + DMSO, respectively; Figure 2A–C). Notably, whereas Wee1 inhibitor II displayed no effects on $Na_v1.2$-mediated I_{Na} in the absence of FGF14, pharmacological inhibition of Wee1 kinase led to an exacerbation of FGF14-mediated suppression of $Na_v1.2$-mediated I_{Na}, as evidenced by HEK-$Na_v1.2$-FGF14-GFP cells treated with Wee1 inhibitor II displaying an average peak I_{Na} density (−29.6 ± 7.29 pA/pF; n = 9) significantly less than HEK-$Na_v1.2$-FGF14-GFP cells treated with vehicle (−89.24 ± 7.7 pA/pF; n = 11; Figure 2A–C). This effect of Wee1 inhibitor II on $Na_v1.2$-mediated peak I_{Na} density is similar to the effect of pharmacological inhibition of Wee1 kinase on tau of fast inactivation of $Na_v1.2$-mediated I_{Na}. Namely, co-expression of FGF14 with the $Na_v1.2$ channel leads to a slowing of the entry of $Na_v1.2$ channels into fast inactivation, as evidenced by the increased tau value observed between the HEK-$Na_v1.2$-GFP + DMSO (0.88 ± 0.10 ms; n = 11) and HEK-$Na_v1.2$-FGF14-GFP + DMSO (1.16 ± 0.08 ms; n = 11) groups, and pharmacological inhibition of Wee1 kinase exacerbates this FGF14-mediated regulatory effects, with the average tau value observed in the HEK-$Na_v1.2$-FGF14-GFP + Wee1 inhibitor II group (2.13 ± 0.35 ms; n = 9) being significantly greater than that observed in the HEK-$Na_v1.2$-FGF14-GFP + DMSO group (1.16 ± 0.08 ms; n = 11; Figure 2D).

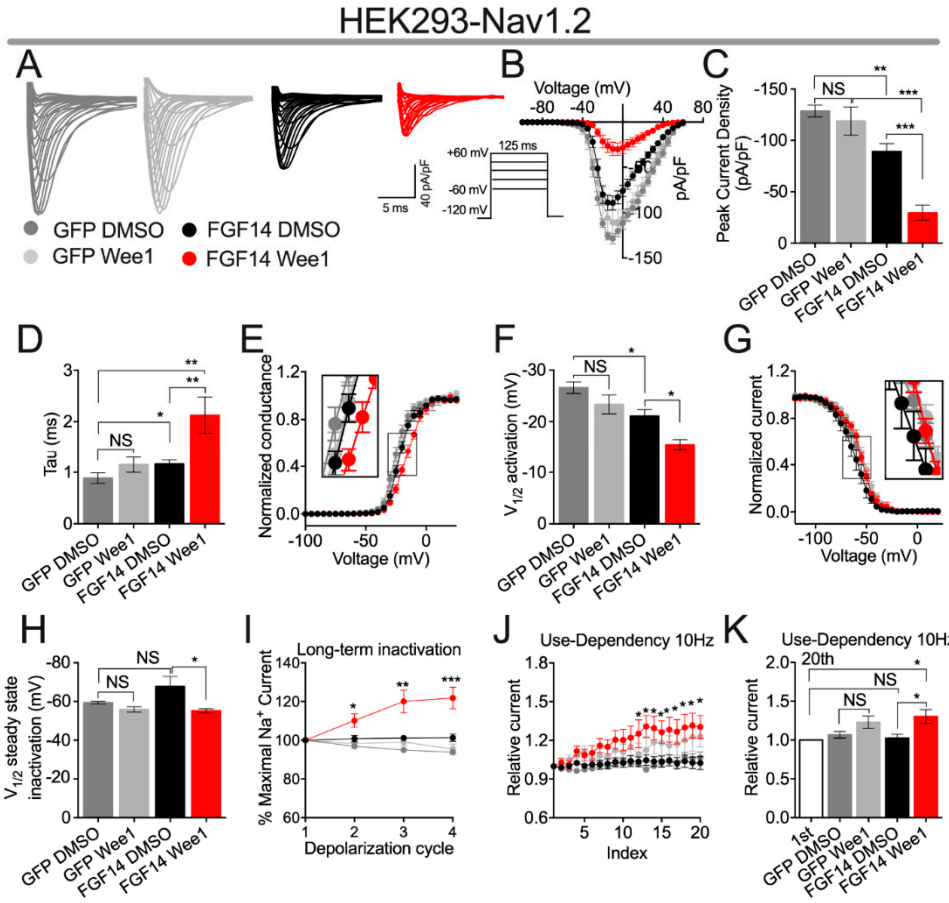

Figure 2. Functional evaluation of the effects of Wee1 inhibitor II on $Na_v1.2$-mediated currents. (**A**) Representative traces of I_{Na} from cells of the indicated experimental groups in the response to the depicted voltage-clamp protocol. (**B**) Current–voltage relationships of cells from the experimental groups described in (**A**). (**C**,**D**) Comparison of peak I_{Na} density (**C**) and the tau of fast inactivation of I_{Na} (**D**) of cells from the indicated experimental groups. (**E**) Normalized conductance plotted as a function of voltage to characterize the voltage-dependence of $Na_v1.2$ channel activation of cells from the experimental groups described in (**A**). Data were fitted with the Boltzmann equation to determine $V_{1/2}$ of activation. (**F**) Bar graph derived from (**E**) comparing $V_{1/2}$ of activation among the indicated experimental groups. (**G**) Normalized current plotted as a function of voltage to characterize the voltage-dependence of $Na_v1.2$ channel steady-state inactivation of cells from the experimental groups described in (**A**). Data were fitted with the Boltzmann equation to determine $V_{1/2}$ of steady-state inactivation. (**H**) Bar graph derived from (**G**) comparing $V_{1/2}$ of $Na_v1.2$ channel steady-state inactivation among the indicated experimental groups. (**I**) Percentage maximal I_{Na} (normalized to the I_{Na} amplitude observed during the first depolarization) plotted as a function of depolarization cycle to characterize the effects of Wee1 inhibitor II on the entry of $Na_v1.2$ channels into long-term inactivation in the experimental groups described in (**A**). (**J**) Relative current (normalized to the I_{Na} amplitude observed during the first depolarization) plotted as a function of depolarization cycle to characterize the effects of pharmacological inhibition of Wee1 kinase on the cumulative inactivation of $Na_v1.2$ channels for the experimental groups described in (**A**). (**K**) Bar graph comparing the ratio of the I_{Na} amplitude observed during the first depolarization normalized to the I_{Na} amplitude observed during the 20th depolarization for the indicated experimental groups. Data are mean ± SEM. Significance was assessed using a one-way ANOVA with post-hoc Tukey's multiple comparisons test. *, $p < 0.05$; **, $p < 0.01$; ***, $p < 0.001$. Data are summarized in Tables 1 and 2.

Consistent with previous investigations [7], co-expression of FGF14 with the $Na_v1.2$ channel led to a depolarizing shift in the voltage-dependence of $Na_v1.2$ channel activation ($V_{1/2}$ of activation = −26.61 ± 1.1 mV (n = 11) and −21.09 ± 1.2 mV (n = 11) for HEK-$Na_v1.2$-GFP + DMSO and HEK-$Na_v1.2$-FGF14-GFP + DMSO, respectively; Figure 2E,F). Similar to the effects of Wee1 inhibitor II on peak I_{Na} density and tau of fast inactivation, pharmacological inhibition of Wee1 displays no effect in the absence of FGF14, but exacerbates FGF14's regulatory effects on the voltage-dependence of $Na_v1.2$ channel acti-

vation, with the average $V_{1/2}$ of activation value observed in the HEK-$Na_v1.2$-FGF14-GFP + Wee1 inhibitor II group (−15.51 ± 0.9 mV; n = 8) being significantly more depolarized relative to that observed in the HEK-$Na_v1.2$-FGF14-GFP + DMSO group (−21.09 ± 1.2 mV; n = 11; Figure 2E,F).

Table 1. Effects of pharmacological inhibition of Wee1 kinase on $Na_v1.2$-mediated currents [†].

Condition	Peak Density	Activation	K_{act}	Steady-State Inactivation	K_{inact}	Tau (τ)
	pA/pF	mV	mV	mV	mV	ms
GFP DMSO	−128.7 ± 5.7 (11)	−26.61 ± 1.1 (11)	4.22 ± 0.4 (11)	−59.32 ± 0.7 (8)	5.17 ± 0.28 (8)	0.88 ± 0.10 (11)
GFP Wee1	−118.8 ± 13.7 (9) [ns]	−23.34 ± 1.8 (9)	4.50 ± 0.3 (9)	−55.92 ± 1.4 (10)	5.38 ± 0.29 (10)	1.15 ± 0.14 (10)
FGF14 DMSO	−89.24 ± 7.7 (11) [a]	−21.09 ± 1.2 (11) [d]	4.47 ± 0.5 (11)	−67.76 ± 5.2 (8)	6.04 ± 0.81 (8)	1.16 ± 0.08 (11) [h]
FGF14 Wee1	−29.6 ± 7.29 (9) [b,c]	−15.51 ± 0.9 (8) [e]	6.58 ± 0.8 (8) [f]	−55.14 ± 1.1 (7) [g]	7.58 ± 0.61 (7)	2.13 ± 0.35 (9) [i]
$FGF14^{Y158A}$ DMSO	−107.3 ± 9.52 (10)	−26.88 ± 1.7 (10)	3.04 ± 0.3 (10)	−51 ± 1.4 (9)	5.76 ± 0.69 (9)	1.65 ± 0.25 (10)
$FGF14^{Y158A}$ Wee1	−124.5 ± 11.4 (11) [ns]	−27.08 ± 2.3 (11)	3.74 ± 0.4 (11)	−49.07 ± 1.2 (11)	5.35 ± 0.50 (10)	1.82 ± 0.32 (11)

[†] Data are mean ± SEM; ns = nonsignificant; (n) = number of cells. [a] p = 0.010, One way ANOVA Tukey's multiple comparisons test compared to GFP DMSO; [b] p = 0.0020, One way ANOVA Tukey's multiple comparisons test compared to FGF14 DMSO; [c] p < 0.0001, One way ANOVA Tukey's multiple comparisons test compared to GFP DMSO; [d] p = 0.029, One way ANOVA Tukey's multiple comparisons test compared to GFP DMSO; [e] p = 0.048, One way ANOVA Tukey's multiple comparisons test compared to FGF14 DMSO; [f] p = 0.020, One way ANOVA Tukey's multiple comparisons test compared to FGF14 DMSO; [g] p = 0.020, One way ANOVA Tukey's multiple comparisons test compared to FGF14 DMSO; [h] p = 0.047, unpaired t tests compared to GFP DMSO; [i] p = 0.0042, One way ANOVA Tukey's multiple comparisons test compared to FGF14 DMSO.

Table 2. Effects of pharmacological inhibition of Wee1 kinase on the entry of $Na_v1.2$ channels into long-term inactivation [†].

Condition	LTI (% Maximal Na^+ Current)		
	2nd Pulse	3rd Pulse	4th Pulse
GFP DMSO	96.87 ± 0.7 (7)	94.95 ± 0.7 (7)	93.82 ± 0.5 (7)
GFP Wee1	98.23 ± 2.3 (10)	99.1 ± 1.9 (10)	95.47 ± 2.6 (10)
FGF14 DMSO	100.8 ± 1.6 (14)	101.2 ± 1.4 (14)	101.3 ± 1.9 (14)
FGF14 Wee1	110.2 ± 3.5 (8) [a]	120 ± 5.8 (8) [b]	121.8 ± 5.5 (8) [c]
$FGF14^{Y158A}$ DMSO	105 ± 2.8 (11)	107.1 ± 4.3 (11)	106.4 ± 3.8 (11)
$FGF14^{Y158A}$ Wee1	103.8 ± 3.4 (9)	108.9 ± 6.4 (9)	107.9 ± 6.5 (9)

[†] Data are mean ± SEM; ns = nonsignificant; (n) = number of cells. [a] p = 0.021, One way ANOVA Tukey's multiple comparisons test compared to FGF14 DMSO; [b] p < 0.0001, One way ANOVA Tukey's multiple comparisons test compared to FGF14 DMSO; [c] p < 0.0001, One way ANOVA Tukey's multiple comparisons test compared to FGF14 DMSO.

Whereas Wee1 inhibitor II exacerbates FGF14-mediated regulation of peak I_{Na} density, tau of fast inactivation, and the voltage-dependence of activation of $Na_v1.2$ channels in heterologous cells, pharmacological inhibition of Wee1 kinase also results in FGF14 displaying entirely altered regulatory on other biophysical properties. Specifically, FGF14 does not inherently modulate the voltage-dependence of $Na_v1.2$ channel steady-state inactivation ($V_{1/2}$ of steady-state inactivation = −59.32 ± 0.7 mV (n = 8) and −67.76 ± 5.2 mV (n = 8) for HEK-$Na_v1.2$-GFP + DMSO and HEK-$Na_v1.2$-FGF14-GFP + DMSO, respectively; Figure 2G,H). However, when Wee1 kinase is pharmacologically inhibited, there is an apparent depolarizing shift in the voltage-dependence of $Na_v1.2$ channel steady-state inactivation observed in the presence of FGF14, as evidenced by the ~12 mV depolarizing shift in this parameter between the HEK-$Na_v1.2$-FGF14-GFP + DMSO (−67.76 ± 5.2 mV; n = 8) and HEK-$Na_v1.2$-FGF14-GFP + Wee1 inhibitor II (−55.14 ± 1.1 mV; n = 7) groups (Figure 2G,H). Notably, no effect of Wee1 inhibitor II is observed on $Na_v1.2$ steady-state

inactivation in the absence of FGF14 (Figure 2G,H), suggesting that this effect is dependent upon the presence of FGF14.

This effect of Wee1 inhibitor II as it relates to entirely altering the function of FGF14 is also evident when investigating how pharmacological inhibition of Wee1 kinase affects long-term and cumulative inactivation of $Na_v1.2$ channels. Specifically, FGF14 does not inherently affect the fraction of $Na_v1.2$ channels that enter into long-term inactivation (Figure 2I; Table 2). Intriguingly, however, HEK-$Na_v1.2$-FGF14-GFP cells treated with Wee1 inhibitor II display a peculiar phenotype in which the I_{Na} amplitude observed during the 2nd, 3rd, and 4th depolarization cycles is significantly larger than that observed during the 1st depolarization cycle, as evidenced by the I_{Na} ratio during the 2nd, 3rd, and 4th depolarization cycles being greater than 100% (Figure 2I; Table 2). Relatedly, FGF14 does not inherently affect the fraction of $Na_v1.2$ channels that undergo cumulative inactivation; however, treatment of HEK-$Na_v1.2$-FGF14-GFP cells with Wee1 kinase inhibitor II results in a phenotype in which the I_{Na} amplitude observed after the 20th pulse is larger than that observed during the 1st pulse (Figure 2J,K). Notably, these effects observed during repetitive stimulation are only present in the HEK-$Na_v1.2$-FGF14-GFP + Wee1 inhibitor II group (Figure 2I–K), suggesting that the phenotype is dependent upon interplay between Wee1 kinase inhibition and FGF14.

3.3. Effects of Wee1 Inhibitor II on FGF14-Mediated Regulation of $Na_v1.2$ Channels Is Depedent upon the Presence of $FGF14^{Y158}$

Previously, we showed that through phosphoryation of $FGF14^{Y158}$, the tyrosine kinase JAK2 modulates FGF14-mediated regulation of Na_v channel activity [14]. As Wee1 is also a tyrosine kinase, and given the robust modulatory effects of pharmacological inhibition of Wee1 on FGF14-mediated regulation of the $Na_v1.2$ channel shown in Figure 2, we next investigated if $FGF14^{Y158}$ was also necessary for Wee1 inhibitor II to exert its regulatory effects on FGF14 activity. To that end, HEK-$Na_v1.2$ cells were transiently transfected with $FGF14^{Y158A}$-GFP (HEK-$Na_v1.2$-$FGF14^{Y158A}$-GFP), and the effects of Wee1 inhibitor II on currents mediated by these cells were assessed using the voltage-clamp protocols employed in Figure 2.

Whereas Wee1 inhibitor II exacerbated FGF14-mediated suppression of $Na_v1.2$-mediated peak I_{Na} density in HEK-$Na_v1.2$-FGF14-GFP cells (Figure 2A–C), pharmacological inhibition of Wee1 kinase had no effect on this parameter when tested in HEK-$Na_v1.2$-$FGF14^{Y158A}$-GFP cells (Figure 3A–C). Relatedly, whereas Wee1 inhibitor II exacerbated FGF14′s effects on tau of fast inactivation (Figure 2D) and the voltage-dependence of activation (Figure 2E,F) of $Na_v1.2$ channels in HEK-$Na_v1.2$-FGF14-GFP cells, the compound did not alter either of these parameters in HEK-$Na_v1.2$-$FGF14^{Y158A}$-GFP cells (Figure 3D–F). Additionally, whereas Wee1 inhibitor II altered the function of FGF14 in HEK-$Na_v1.2$-FGF14-GFP cells and induced a depolarizing shift in the voltage-dependence of $Na_v1.2$ channel steady-state inactivation in the presence of FGF14 (Figure 2G,H), pharmacological inhibition of Wee1 kinase had no effects on this parameter in the presence of $FGF14^{Y158A}$ (Figure 3G,H).

In the presence of FGF14, Wee1 inhibitor II also exerted a peculiar effect on the long-term and cumulative inactivation of $Na_v1.2$ channels that was characterized by an increase in the amplitude of I_{Na} after repetitive stimulation (Figure 2I–K). In HEK-$Na_v1.2$-$FGF14^{Y158A}$-GFP cells, however, the ratio of I_{Na} amplitude (normalized to the I_{Na} amplitude observed during the first depolarization) of the 2nd, 3rd, and 4th depolarizations cycles was not different in the long-term inactivation protocol when comparing HEK-$Na_v1.2$-$FGF14^{Y158A}$-GFP cells treated with vehicle to HEK-$Na_v1.2$-$FGF14^{Y158A}$-GFP cells treated with Wee1 inhibitor II (Figure 3I). Relatedly, the ratio of I_{Na} amplitude (normalized to the I_{Na} amplitude observed during the first depolarization) was not different for any of the depolarization cycles in the cumulative inactivation protocol for HEK-$Na_v1.2$-$FGF14^{Y158A}$-GFP cells treated with vehicle versus HEK-$Na_v1.2$-$FGF14^{Y158A}$-GFP cells treated with Wee1 inhibitor II (Figure 3J,K). Interestingly, however, HEK-$Na_v1.2$-$FGF14^{Y158A}$-GFP cells

treated with both vehicle and Wee1 inhibitor II displayed larger I_{Na} amplitudes after repetitive stimulation compared to their I_{Na} amplitudes observed after the first depolarization cycle (Figure 3K).

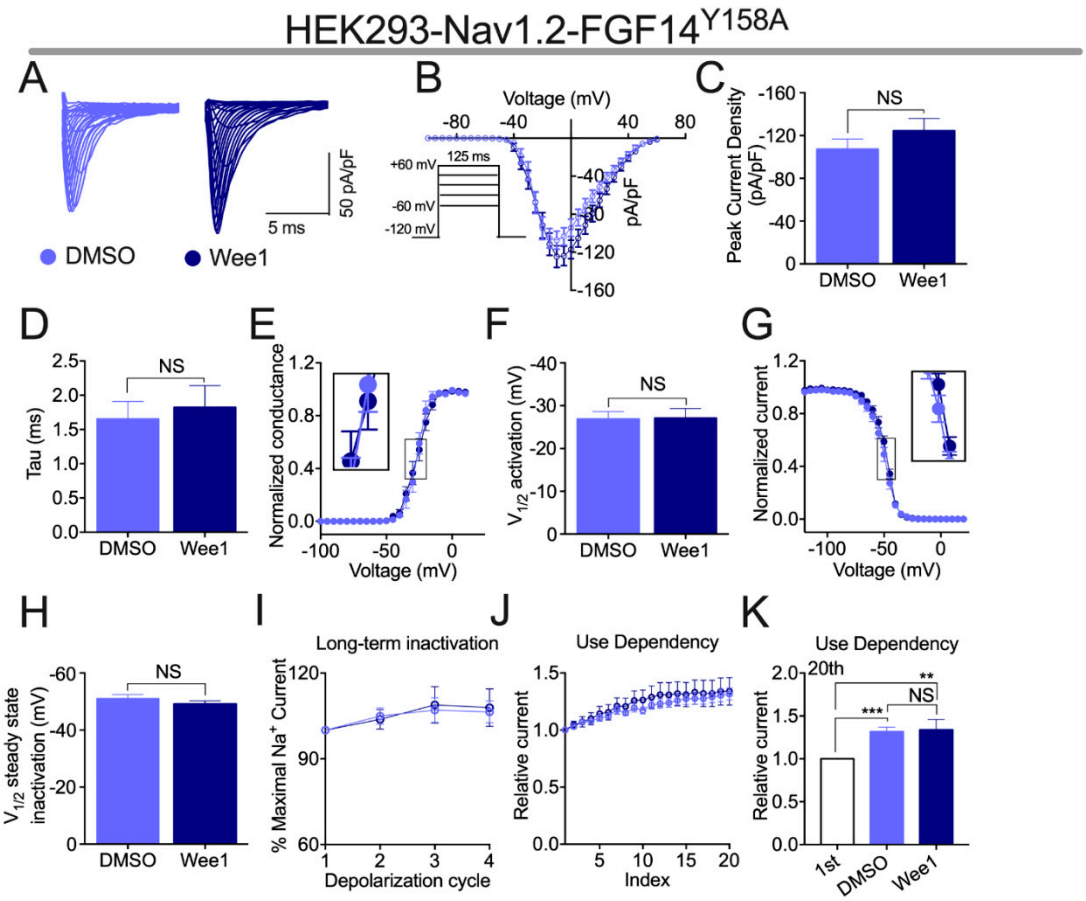

Figure 3. Functional evaluation of the effects of Wee1 inhibitor II in HEK-$Na_v1.2$ cells co-expressing $FGF14^{Y158A}$. (**A**) Representative traces of I_{Na} elicited by cells from the indicated experimental groups in response to the depicted voltage-clamp protocol. (**B**) Current–voltage relationship of cells from the experimental groups described in (**A**). (**C**) Comparison of the peak I_{Na} density of cells of the indicated experimental groups. (**D**) Comparison of tau of $Na_v1.2$ channel fast inactivation between the indicated experimental groups. (**E**) Conductance–voltage relationship of $Na_v1.2$ channels in the experimental groups described in (**A**). (**F**) Comparison of $V_{1/2}$ of $Na_v1.2$ channel activation between the indicated experimental groups. (**G**) Normalized current plotted as a function of voltage to characterize the voltage-dependence of $Na_v1.2$ channel steady-state inactivation for the experimental groups described in (**A**). (**H**) Comparison of $V_{1/2}$ of $Na_v1.2$ channel steady-state inactivation between the indicated experimental groups. (**I**,**J**) Characterization of long-term inactivation (**I**) and cumulative inactivation (**J**) of $Na_v1.2$ channels for the experimental groups described in (**A**). (**K**) Comparison of the relative I_{Na} amplitude at the 1st pulse to the 20th pulse for the indicated experimental groups. Data are mean ± SEM. Significance was assessed using a one-way ANOVA with post hoc Tukey's multiple comparisons test. **, $p < 0.01$; ***, $p < 0.001$. Data are summarized in Tables 1 and 2.

3.4. Wee1 Inhibitor II Does Not Affect FGF14-Mediated Regulation of the $Na_v1.6$ Channel

Having shown in our LCA experiments that Wee1 inhibitor II did not affect FGF14:$Na_v1.6$ complex assembly (Figure 1C), we next sought to investigate if, and unlike the modulatory of Wee1 inhibitor II on FGF14-mediated regulatory effects of the $Na_v1.2$ channel (Figure 2), this would preclude the ligand from conferring functional modulation of the $Na_v1.6$ channel or FGF14:$Na_v1.6$ complex. To do so, HEK293 cells stably expressing the $Na_v1.6$ channel (HEK-$Na_v1.6$) were transiently transfected with either GFP (HEK-$Na_v1.6$-GFP) or FGF14-GFP (HEK-$Na_v1.6$-FGF14-GFP). Cells were incubated for 30 min prior to recording with

either vehicle (0.1% DMSO) or 15 μM Wee1 inhibitor II, and the voltage-clamp protocols employed in Figures 2 and 3 were used to characterize effects of pharmacological inhibition of Wee1 kinase on $Na_v1.6$ channel activity (Figure 4; Tables 3 and 4).

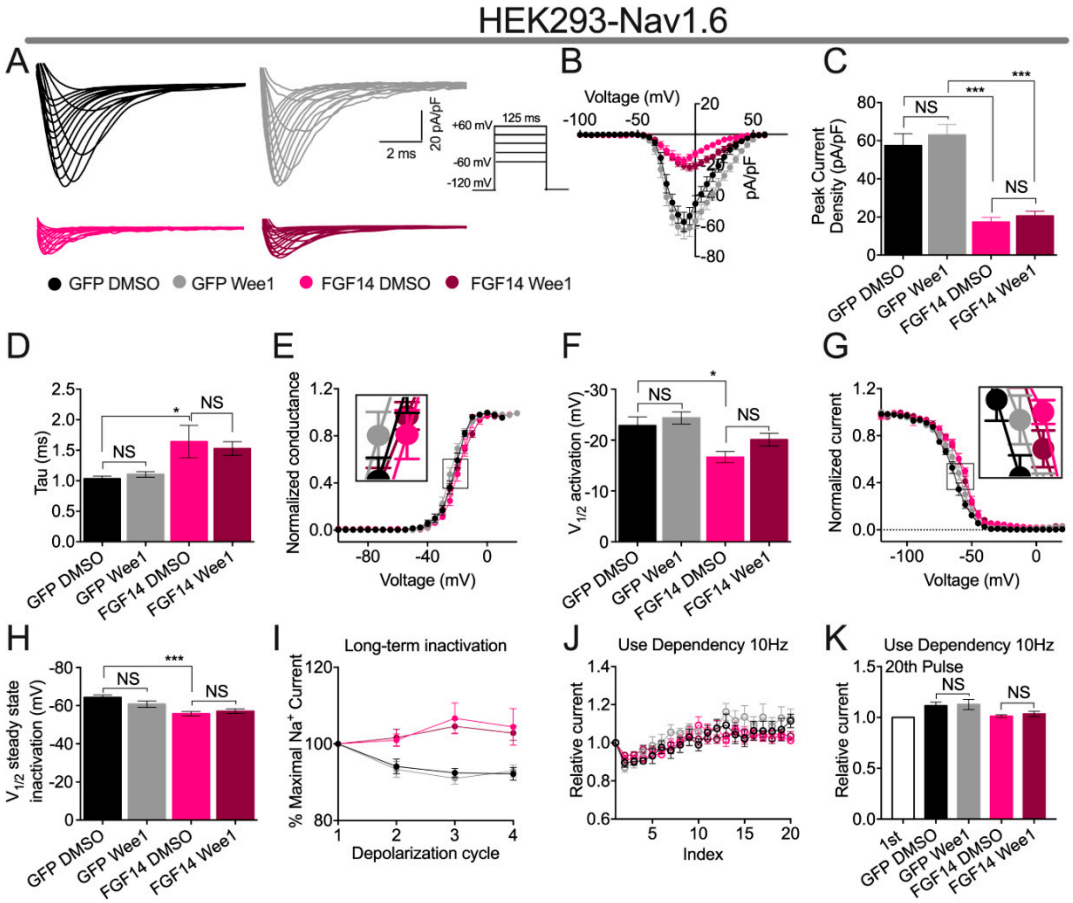

Figure 4. Wee1 inhibitor II does not affect FGF14-mediated regulation of the $Na_v1.6$ channel. (**A**) Representative traces of I_{Na} elicited by cells of the indicated experimental groups in response to the depicted voltage-clamp protocol. (**B**) Current–voltage relationships of cells from the experimental groups described in (**A**). (**C**) Peak I_{Na} density of cells from the indicated experimental groups. (**D**) Tau of fast inactivation of cells from the indicated experimental groups. (**E**) Voltage-dependence of activation of cells from the experimental groups described in (**A**). (**F**) $V_{1/2}$ of activation of cells from the indicated experimental groups. (**G**) Steady-state inactivation plots of cells from the experimental groups described in (**A**). (**H**) $V_{1/2}$ of steady-state inactivation of cells from the indicated experimental groups. (**I**) Characterization of entry of $Na_v1.6$ channels into long-term inactivation for the experimental groups described in (**A**). (**J**) Characterization of cumulative inactivation of $Na_v1.6$ channels for the experimental groups described in (**A**). (**K**) Relative current at the 20th pulse (normalized to the I_{Na} amplitude observed during the first depolarization) for the indicated experimental groups. Data are mean ± SEM. Significance was assessed using a one-way ANOVA with post hoc Tukey's multiple comparisons test. *, $p < 0.05$; ***, $p < 0.001$. Data are summarized in Tables 3 and 4.

Consistent with the results of previous investigations [14,25–28,30], co-expression of FGF14 with the $Na_v1.6$ channel in heterologous cells lead to a reduction in the peak I_{Na} density of $Na_v1.6$-mediated currents, as evidenced by HEK-$Na_v1.6$-FGF14-GFP cells displaying an average peak I_{Na} density (-17.31 ± 2.5 pA/pF; $n = 10$) significantly less than HEK-$Na_v1.6$-GFP cells (-57.83 ± 6.3 pA/pF; $n = 8$; Figure 4A–C). Whereas Wee1 inhibitor II exacerbated this FGF14-mediated regulatory on $Na_v1.2$-mediated currents (Figure 2A–C), pharmacological inhibition of Wee1 kinase did not affect $Na_v1.6$-mediated peak I_{Na} density in the absence or presence of FGF14 (Figure 4A–C).

Table 3. Effects of pharmacological inhibition of Wee1 kinase on $Na_v1.6$-mediated currents [†].

Condition	Peak Density	Activation	K_{act}	Steady-State Inactivation	K_{inact}	Tau (τ)
	pA/pF	mV	mV	mV	mV	ms
GFP DMSO	−57.38 ± 6.3 (8)	−22.87 ± 1.69 (8)	4.79 ± 0.46 (8)	−60.4 ± 1.67 (8)	5.93 ± 0.48 (8)	1.03 ± 0.04 (8)
GFP Wee1	−62.99 ± 5.5 (8)	−24.38 ± 1.19 (8)	4.29 ± 0.43 (8)	−60.84 ± 1.67 (8)	6.15 ± 0.40 (8)	1.11 ± 0.04 (8)
FGF14 DMSO	−17.31 ± 2.5 (10) [a]	−18.15 ± 1.03 (8) [c]	5.05 ± 0.51 (8)	−55.77 ± 1.10 (8) [d]	5.654 ± 0.57 (8)	1.64 ± 0.26 (8) [e]
FGF14 Wee1	−20.57 ± 2.5 (10) [ns,b]	−20.11 ± 1.25 (8)	5.89 ± 0.57 (8)	−57.12 ± 1.19 (8)	6.91 ± 0.80 (7)	1.53 ± 0.11 (9)

[†] Data are mean ± SEM; ns = nonsignificant; (*n*) = number of cells. [a] $p < 0.0001$, One way ANOVA Tukey's multiple comparisons test compared to GFP DMSO; [b] $p < 0.0001$, One way ANOVA Tukey's multiple comparisons test compared to GFP Wee1; [c] $p = 0.012$, One way ANOVA Tukey's multiple comparisons test compared to GFP DMSO; [d] $p = 0.00090$, One way ANOVA Tukey's multiple comparisons test compared to GFP DMSO; [e] $p = 0.0328$, One way ANOVA Tukey's multiple comparisons test compared to GFP DMSO.

Table 4. Effects of Wee1 inhibitor II on entry of $Na_v1.6$ channels into long-term inactivation [†].

Condition	LTI (% Maximal Na^+ Current)		
	2nd Pulse	3rd Pulse	4th Pulse
GFP DMSO	94.11 ± 1.9 (8)	92.43 ± 1.3 (8)	92.18 ± 1.6 (8)
GFP Wee1	93.35 ± 2.1 (9)	91.02 ± 1.5 (9)	92.94 ± 1.5 (9)
FGF14 DMSO	101.0 ± 1.6 (8) [a]	106.7 ± 4.0 (8) [b]	104.5 ± 4.7 (8) [c]
FGF14 Wee1	101.7 ± 2.2 (8)	104.6 ± 1.7 (8)	102.9 ± 1.9 (8)

[†] Data are mean ± SEM; ns = nonsignificant; (*n*) = number of cells; [a] $p = 0.0159$, unpaired *t* tests compared to GFP DMSO; [b] $p = 0.0012$, One way ANOVA Tukey's multiple comparisons test compared to GFP DMSO; [c] $p = 0.0021$, One way ANOVA Tukey's multiple comparisons test compared to GFP DMSO.

Consistent with previous investigations [14,25–28,30], co-expression of FGF14 with the $Na_v1.6$ channel lead to a slowing of $Na_v1.6$ channel fast inactivation (Figure 4D) and a depolarizing shift in the voltage-dependence of $Na_v1.6$ channel activation (Figure 4E,F). These findings are evidenced by HEK-$Na_v1.6$-GFP cells displaying a tau of fast inactivation of 1.03 ± 0.04 ms ($n = 8$), whereas HEK-$Na_v1.6$-FGF14-GFP cells display a significantly larger value for this parameter of 1.64 ± 0.26 ms ($n = 8$; Figure 4D), and HEK-$Na_v1.6$-GFP cells displaying a $V_{1/2}$ of activation of −22.87 ± 1.69 mV ($n = 8$), whereas HEK-$Na_v1.6$-FGF14-GFP cells display a significantly more depolarized $V_{1/2}$ of activation of −18.15 ± 1.03 mV ($n = 8$; Figure 4E,F), respectively. Whereas Wee1 inhibitor II exacerbated FGF14-mediated regulatory effects on the tau of fast inactivation and the voltage-dependence of activation of $Na_v1.2$ channels (Figure 2D–F), pharmacological inhibition of Wee1 kinase did not affect the tau of fast of inactivation or the voltage-dependence of activation of $Na_v1.6$ channels in the absence of presence of FGF14 (Figure 4D–F). Relatedly, whereas Wee1 inhibitor II entirely altered the regulatory effects of FGF14 on steady-state inactivation, namely, inducing a depolarizing shift in the $V_{1/2}$ of $Na_v1.2$ steady-state inactivation despite FGF14 not inherently regulating this parameter of $Na_v1.2$ channels (Figure 2G,H), pharmacological inhibition of Wee1 kinase did not affect the voltage-dependence of $Na_v1.6$ steady-state inactivation in the absence or presence of FGF14 (Figure 4G,H). This finding is particularly notable on account of FGF14's differential regulation of the voltage-dependence of steady-state inactivation of $Na_v1.2$ versus $Na_v1.6$, where FGF14 does not modulate this parameter of $Na_v1.2$ channels (Figure 2G,H), but confers a depolarizing shift in the voltage-dependence of $Na_v1.6$ channel steady state-inactivation (Figure 4G,H) when the two proteins are co-expressed in heterologous cells, which is a finding consistent with previous investigations [7].

As also observed in previous studies [14,30], co-expression of FGF14 with the $Na_v1.6$ channel in heterologous cells resulted in a reduction in the fraction of $Na_v1.6$ channels entering into long-term inactivation (Figure 4I). This is evidenced by the I_{Na} ratio (normalized to the I_{Na} amplitude during the first depolarization) of 2nd, 3rd, and 4th depolarization

cycles being greater in HEK-$Na_v1.6$-FGF14-GFP cells compared to HEK-$Na_v1.6$-GFP cells (Figure 4I; Table 4). However, Wee1 inhibitor II did not affect the entry of $Na_v1.6$ channels into long-term inactivation in the absence or presence of FGF14 (Figure 4I; Table 4). Similarly, pharmacological inhibition of Wee1 kinase did not affect the cumulative inactivation of $Na_v1.6$ channels in the absence or presence of FGF14 (Figure 4J,K).

4. Discussion

Intracellular fibroblast growth factors (iFGF; FGF11-FGF14) have emerged as important Na_v channel auxiliary proteins [6–8,10,35–40]. Notably, PPIs between different iFGFs and different Na_v channel isoforms contribute to the generation of phenotypically distinct sodium currents with specialized functions in different tissues [7,9,37,41–43]. For example, the PPI between FGF12 and the $Na_v1.5$ channel confers important regulatory effects on the I_{Na} of cardiomyocytes [41,42]; the PPI between FGF13 and the $Na_v1.7$ channel confers important regulatory effects on the I_{Na} of dorsal root ganglion neurons [9,43,44]; and the PPI between FGF14 and the $Na_v1.2$ and $Na_v1.6$ channel is important for regulating the I_{Na} and excitability of hippocampal and striatal neurons [7,14,26,37,45]. Despite these diverse and well-established regulatory effects of iFGFs on Na_v channels, less is known about cellular signaling molecules that might regulate and enable the targeted modulation conferred by different iFGFs on different Na_v channel isoforms. To that end, and focusing on the PPI between FGF14 and the $Na_v1.2$ channel and $Na_v1.6$ channel given the primacy of these PPIs in regulating neuronal Na+ currents and excitability [7,11,12,14,26,27,37,45], we built upon previous studies suggesting a potential role of Wee1 kinase in modulating FGF14-mediated regulation of central nervous system Na_v channel isoforms [13,14,17].

In our previous studies investigating kinase networks that might regulate Na_v channel macromolecular complexes, evidence emerged of an intricate pathway involving GSK3, AKT, and Wee1 that might regulate Na_v channel activity and neuronal excitability [13,17]. Supporting such a hypothesis, we have previously shown that GSK3-mediated phosphorylation of T1966 of $Na_v1.2$ and T1936 of $Na_v1.6$ confers important regulatory effects on the biophysical properties of these channels and on the excitability of neurons in clinically relevant brain regions [16,29]. Additionally, we have shown that AKT is an important regulator of repetitive firing of hippocampal and striatal neurons [16,17]. Given that Wee1 kinase is regulated and degraded by GSK3 through ubiquitination [19–21], and that Wee1 kinase may increase the activity of AKT [22], which would be predicted to, in turn, inhibit GSK3 activity [17], we sought in this work to take a focused approach toward unraveling the complex role of Wee1 in regulating this kinase network.

In a previous study, Wee1 inhibitor II was identified as the most targeted pharmacological inhibitor of Wee1 kinase [34]. Using this chemical tool, we tested the effects of pharmacological inhibition of Wee1 kinase in our previously described LCA optimized to identify modulators of complex's involving iFGFs and Na_v channels [15,23]. When tested for modulatory effects on FGF14:$Na_v1.2$ complex assembly (Figure 1A), Wee1 inhibitor II was shown to demonstrate dose-dependent inhibition of the complex's formation. This finding could suggest that Wee1 kinase phosphorylates residues at the FGF14:$Na_v1.2$ PPI interface that are important for complex assembly. Supporting such a hypothesis, when the effects of Wee1 inhibitor II on FGF14:$Na_v1.2$ complex assembly were assayed in conditions featuring $FGF14^{Y158A}$, which represents an FGF14 point mutation previously shown to abrogate phosphorylation-mediated regulation of FGF14 by JAK2 [14], the compound failed to exert noticeable effects of FGF14:$Na_v1.2$ complex assembly (Figure 1B). This finding could suggest that Wee1 kinase exerts its modulatory effects on FGF14:$Na_v1.2$ complex assembly through phosphorylation of $FGF14^{Y158}$; however, future in vitro phosphorylation assays that demonstrate phosphorylation of $FGF14^{Y158}$ by Wee1 kinase are necessary to unequivocally substantiate such a hypothesis.

In contrast to the modulatory effects on FGF14:$Na_v1.2$ complex assembly exerted by Wee1 inhibitor II, the compound did not exert noticeable effects on FGF14:$Na_v1.6$ complex assembly in our LCA experiments (Figure 1C). This lack of appreciable effects of Wee1 in-

hibitor II on FGF14:$Na_v1.6$ complex assembly is consistent with previous investigations [13]. However, in our previous study, Wee1 inhibitor I (chemical name: 4-(2-Chlorophenyl)−9-hydroxypyrrolo[3,4-c]carbazole-1,3(2H,6H)-dione; referred to as compound 23 when initially disclosed [34]) did exert appreciable inhibitory effects on FGF14:$Na_v1.6$ complex assembly at high micromolar concentrations [13]. Given that Wee1 inhibitor I was previously shown to be less selective for kinases related to Wee1 kinase compared to Wee1 inhibitor II [34], these differential effects of the two compounds on FGF14:$Na_v1.6$ complex assembly are presumed to arise due to the different selectivity profiles of the two compounds, with the inhibitory effects of Wee1 inhibitor I conferred on FGF14:$Na_v1.6$ complex assembly presumed to be due to off-target modulation of other kinases.

Having shown that Wee1 inhibitor II exerts robust modulatory effects on FGF14:$Na_v1.2$ complex assembly, we next sought to investigate if pharmacological inhibition of Wee1 kinase would alter FGF14-mediated regulation of the $Na_v1.2$ channel. In support of Wee1 kinase conferring modulatory effects on FGF14-mediated regulation of the $Na_v1.2$ channel, Wee1 inhibitor II displayed effects on $Na_v1.2$ mediated currents, but only in the presence of FGF14. In particular, pharmacological inhibition of Wee1 kinase was shown to exacerbate FGF14-mediated regulatory effects on some electrophysiological parameters of the $Na_v1.2$ channel (i.e., peak I_{Na} density, tau of fast inactivation, and voltage-dependence of activation) and entirely alter FGF14 activity with respect to other electrophysiological parameters. As it pertains to the latter, Wee1 inhibitor II, in the presence of FGF14, lead to a depolarizing shift in the voltage-dependence of $Na_v1.2$ channel steady-state inactivation, an electrophysiological parameter that is not inherently modulated by FGF14 (Figure 2G,H). Likewise, pharmacological inhibition of Wee1 kinase resulted in an increased I_{Na} amplitude after repetitive simulation (when compared to the I_{Na} amplitude observed during the first depolarization cycle of either the long-term inactivation or cumulative inactivation protocols; Figure 2I–K), which are also not regulatory effects inherent to FGF14. Collectively, these findings suggest that Wee1 kinase confers complex regulatory effects on the $Na_v1.2$ channel by altering the activity of FGF14.

To elucidate molecular determinants of how Wee1 kinase alters FGF14-mediated regulation of the $Na_v1.2$ channel, and based upon the LCA data shown in Figure 1B, we tested Wee1 inhibitor II in HEK-$Na_v1.2$ cells co-expressing $FGF14^{Y158A}$ (Figure 3). In contrast to the myriad of effects of Wee1 inhibitor II on FGF14-mediated regulation of the $Na_v1.2$ channel in the presence of WT FGF14 (Figure 2), pharmacological inhibition of Wee1 kinase did not confer any changes in FGF14-mediated regulation of the $Na_v1.2$ channel in the presence of $FGF14^{Y158A}$. Coupled with the LCA data shown in Figure 1B, these functional data provide strong evidence for $FGF14^{Y158}$ being an important residue that confers Wee1 with its regulatory effects on the $Na_v1.2$ channel macromolecular complex.

Given that FGF14 has previously been shown to confer differential modulation of the $Na_v1.2$ and $Na_v1.6$ channels, coupled with the lack of effect of Wee1 inhibitor II on FGF14:$Na_v1.6$ complex assembly in the LCA experiments (Figure 1C), we lastly investigated if pharmacological inhibition of Wee1 kinase might confer different functional effects on FGF14-mediated regulation of the $Na_v1.2$ channel versus $Na_v1.6$ channel. Consistent with the LCA experiments showing no effects of Wee1 inhibitor II on FGF14:$Na_v1.6$ complex assembly (Figure 1C), pharmacological inhibition of Wee1 kinase did not affect $Na_v1.6$-mediated Na+ currents in the absence or presence of FGF14 (Figure 4). Collectively considered, these data suggest that there could be residues at the FGF14:$Na_v1.2$ PPI interface that are targeted by Wee1 kinase that are not conserved among other iFGF:Na_v channel pairs; although, extensive structural and biophysical investigations would be necessary to unequivocally substantiate such suppositions.

Overall, by complementarily employing the LCA and whole-cell patch-clamp electrophysiology in heterologous cells, we have demonstrated that pharmacological inhibition of Wee1 kinase confers modulatory effects on the $Na_v1.2$, but not the $Na_v1.6$, macromolecular complex. As both of these Na_v channel isoforms are enriched in clinically relevant brain re-

gions with different subcellular distributions [46], our findings have important implications for understanding cellular signaling molecules that fine-tune neuronal excitability.

In particular, and given the selective effects of Wee1 inhibitor II on FGF14-mediated regulation of the $Na_V1.2$ channel, but not the $Na_V1.6$ channel, our data suggest that Wee1 kinase could confer targeted subcellular regulation of neuronal activity. Such a hypothesis is supported by $Na_V1.2$ channels being enriched in the somatodendritic region and proximal axon initial segment of neurons where they contribute to action potential backpropagation and spike timing-dependent plasticity, whereas $Na_V1.6$ channels are enriched in the distal region of the axon initial segment where they contribute to the forward propagation of action potentials and repetitive firing [46–49]. As such, our data suggest that Wee1 kinase might have an important role in promoting action potential backpropagation and synaptic signal integration, although, future ex vivo current-clamp recordings would be necessary to validate such regulatory mechanisms [47].

Author Contributions: Conceptualization, N.M.D., C.M.T., F.L. and A.K.S.; methodology, N.M.D., C.M.T., F.L. and A.K.S.; validation, F.L. and A.K.S.; formal analysis, N.M.D., C.M.T. and A.K.S.; investigation, N.M.D., C.M.T., J.S., T.J.B. and A.K.S.; resources, F.L. and A.K.S.; data curation, N.M.D., C.M.T. and A.K.S.; writing—original draft preparation, N.M.D.; writing—N.M.D., C.M.T., F.L. and A.K.S.; visualization, N.M.D., C.M.T. and A.K.S.; supervision, F.L. and A.K.S.; project administration, F.L.; funding acquisition, F.L. All authors have read and agreed to the published version of the manuscript.

Funding: This work was supported by the Houston Area Molecular Biophysics Program Grant No. T32 GM008280 (N.M.D.), UTMB Department of Neurology Training Program funded by The National Institute of Aging (NIH Grant # T32AG067952-01; T.J.B.), National Institute of Environmental Health Sciences T32-ES007254 (C.M.T.), National Institutes of Health Grants R01MH12435101 (F.L.).

Institutional Review Board Statement: Not applicable.

Informed Consent Statement: Not applicable.

Data Availability Statement: Data included in this study are available upon request from the corresponding author.

Acknowledgments: We acknowledge the Sealy Center for Structural Biology and Molecular Biology at the University of Texas Medical Branch at Galveston for providing research resources.

Conflicts of Interest: The authors declare no conflict of interest.

References

1. Catterall, W.A. Forty Years of Sodium Channels: Structure, Function, Pharmacology, and Epilepsy. *Neurochem. Res.* **2017**, *42*, 2495–2504. [CrossRef]
2. Catterall, W.A. From Ionic Currents to Molecular Mechanisms: The Structure and Function of Voltage-Gated Sodium Channels. *Neuron* **2000**, *26*, 13–25. [CrossRef]
3. Catterall, W.A.; Swanson, T.M. Structural Basis for Pharmacology of Voltage-Gated Sodium and Calcium Channels. *Mol. Pharmacol.* **2015**, *88*, 141–150. [CrossRef] [PubMed]
4. Tseng, T.-T.; McMahon, A.M.; Johnson, V.T.; Mangubat, E.Z.; Zahm, R.J.; Pacold, M.E.; Jakobsson, E. Sodium Channel Auxiliary Subunits. *J. Mol. Microbiol. Biotechnol.* **2007**, *12*, 249–262. [CrossRef]
5. Pitt, G.S.; Lee, S.-Y. Current View on Regulation of Voltage-Gated Sodium Channels by Calcium and Auxiliary Proteins. *Protein Sci.* **2016**, *25*, 1573–1584. [CrossRef]
6. Lou, J.-Y.; Laezza, F.; Gerber, B.R.; Xiao, M.; Yamada, K.A.; Hartmann, H.; Craig, A.M.; Nerbonne, J.M.; Ornitz, D.M. Fibroblast Growth Factor 14 Is an Intracellular Modulator of Voltage-Gated Sodium Channels. *J. Physiol.* **2005**, *569*, 179–193. [CrossRef] [PubMed]
7. Laezza, F.; Lampert, A.; Kozel, M.A.; Gerber, B.R.; Rush, A.M.; Nerbonne, J.M.; Waxman, S.G.; Dib-Hajj, S.D.; Ornitz, D.M. FGF14 N-Terminal Splice Variants Differentially Modulate $Na_V1.2$ and $Na_V1.6$-Encoded Sodium Channels. *Mol. Cell. Neurosci.* **2009**, *42*, 90–101. [CrossRef] [PubMed]
8. Goetz, R.; Dover, K.; Laezza, F.; Shtraizent, N.; Huang, X.; Tchetchik, D.; Eliseenkova, A.V.; Xu, C.-F.; Neubert, T.A.; Ornitz, D.M.; et al. Crystal Structure of a Fibroblast Growth Factor Homologous Factor (FHF) Defines a Conserved Surface on FHFs for Binding and Modulation of Voltage-Gated Sodium Channels. *J. Biol. Chem.* **2009**, *284*, 17883–17896. [CrossRef] [PubMed]

9. Effraim, P.R.; Huang, J.; Lampert, A.; Stamboulian, S.; Zhao, P.; Black, J.A.; Dib-Hajj, S.D.; Waxman, S.G. Fibroblast Growth Factor Homologous Factor 2 (FGF-13) Associates with $Na_v1.7$ in DRG Neurons and Alters Its Current Properties in an Isoform-Dependent Manner. *Neurobiol. Pain* **2019**, *6*, 100029. [CrossRef]
10. Wittmack, E.K.; Rush, A.M.; Craner, M.J.; Goldfarb, M.; Waxman, S.G.; Dib-Hajj, S.D. Fibroblast Growth Factor Homologous Factor 2B: Association with $Na_v1.6$ and Selective Colocalization at Nodes of Ranvier of Dorsal Root Axons. *J. Neurosci.* **2004**, *24*, 6765–6775. [CrossRef]
11. White, H.V.; Brown, S.T.; Bozza, T.C.; Raman, I.M. Effects of FGF14 and NaVβ4 Deletion on Transient and Resurgent Na Current in Cerebellar Purkinje Neurons. *J. Gen. Physiol.* **2019**, *151*, 1300–1318. [CrossRef] [PubMed]
12. Yan, H.; Pablo, J.L.; Wang, C.; Pitt, G.S. FGF14 Modulates Resurgent Sodium Current in Mouse Cerebellar Purkinje Neurons. *eLife* **2014**, *3*, e04193. [CrossRef] [PubMed]
13. Hsu, W.-C.; Nenov, M.N.; Shavkunov, A.; Panova, N.; Zhan, M.; Laezza, F. Identifying a Kinase Network Regulating FGF14:$Na_v1.6$ Complex Assembly Using Split-Luciferase Complementation. *PLoS ONE* **2015**, *10*, e0117246. [CrossRef]
14. Wadsworth, P.A.; Singh, A.K.; Nguyen, N.; Dvorak, N.M.; Tapia, C.M.; Russell, W.K.; Stephan, C.; Laezza, F. JAK2 Regulates $Na_v1.6$ Channel Function via FGF14(Y158) Phosphorylation. *Biochim. Biophys. Acta (BBA)-Mol. Cell Res.* **2020**, *1867*, 118786. [CrossRef] [PubMed]
15. Wadsworth, P.A.; Folorunso, O.; Nguyen, N.; Singh, A.K.; D'Amico, D.; Powell, R.T.; Brunell, D.; Allen, J.; Stephan, C.; Laezza, F. High-Throughput Screening against Protein:Protein Interaction Interfaces Reveals Anti-Cancer Therapeutics as Potent Modulators of the Voltage-Gated Na(+) Channel Complex. *Sci. Rep.* **2019**, *9*, 16890. [CrossRef] [PubMed]
16. Scala, F.; Nenov, M.N.; Crofton, E.J.; Singh, A.K.; Folorunso, O.; Zhang, Y.; Chesson, B.C.; Wildburger, N.C.; James, T.F.; Alshammari, M.A.; et al. Environmental Enrichment and Social Isolation Mediate Neuroplasticity of Medium Spiny Neurons through the GSK3 Pathway. *Cell Rep.* **2018**, *23*, 555–567. [CrossRef]
17. Di Re, J.; Hsu, W.-C.J.; Kayasandik, C.B.; Fularczyk, N.; James, T.F.; Nenov, M.N.; Negi, P.; Marosi, M.; Scala, F.; Prasad, S.; et al. Inhibition of AKT Signaling Alters BIV Spectrin Distribution at the AIS and Increases Neuronal Excitability. *Front. Mol. Neurosci.* **2021**, *14*, 128. [CrossRef] [PubMed]
18. Matheson, C.J.; Backos, D.S.; Reigan, P. Targeting WEE1 Kinase in Cancer. *Trends Pharmacol. Sci.* **2016**, *37*, 872–881. [CrossRef]
19. Watanabe, N.; Arai, H.; Nishihara, Y.; Taniguchi, M.; Watanabe, N.; Hunter, T.; Osada, H. M-Phase Kinases Induce Phospho-Dependent Ubiquitination of Somatic Wee1 by SCFbeta-TrCP. *Proc. Natl. Acad. Sci. USA* **2004**, *101*, 4419–4424. [CrossRef]
20. Li, V.S.W.; Ng, S.S.; Boersema, P.J.; Low, T.Y.; Karthaus, W.R.; Gerlach, J.P.; Mohammed, S.; Heck, A.J.R.; Maurice, M.M.; Mahmoudi, T.; et al. Wnt Signaling through Inhibition of β-Catenin Degradation in an Intact Axin1 Complex. *Cell* **2012**, *149*, 1245–1256. [CrossRef]
21. Penas, C.; Mishra, J.K.; Wood, S.D.; Schürer, S.C.; Roush, W.R.; Ayad, N.G. GSK3 Inhibitors Stabilize Wee1 and Reduce Cerebellar Granule Cell Progenitor Proliferation. *Cell Cycle* **2015**, *14*, 417–424. [CrossRef]
22. Cen, L.; Carlson, B.L.; Schroeder, M.A.; Ostrem, J.L.; Kitange, G.J.; Mladek, A.C.; Fink, S.R.; Decker, P.A.; Wu, W.; Kim, J.-S.; et al. P16-Cdk4-Rb Axis Controls Sensitivity to a Cyclin-Dependent Kinase Inhibitor PD0332991 in Glioblastoma Xenograft Cells. *Neuro-Oncology* **2012**, *14*, 870–881. [CrossRef] [PubMed]
23. Shavkunov, A.; Panova, N.; Prasai, A.; Veselenak, R.; Bourne, N.; Stoilova-McPhie, S.; Laezza, F. Bioluminescence Methodology for the Detection of Protein-Protein Interactions within the Voltage-Gated Sodium Channel Macromolecular Complex. *Assay Drug Dev. Technol.* **2012**, *10*, 148–160. [CrossRef] [PubMed]
24. Shavkunov, A.S.; Wildburger, N.C.; Nenov, M.N.; James, T.F.; Buzhdygan, T.P.; Panova-Elektronova, N.I.; Green, T.A.; Veselenak, R.L.; Bourne, N.; Laezza, F. The Fibroblast Growth Factor 14·voltage-Gated Sodium Channel Complex Is a New Target of Glycogen Synthase Kinase 3 (GSK3). *J. Biol. Chem.* **2013**, *288*, 19370–19385. [CrossRef] [PubMed]
25. Ali, S.R.; Singh, A.K.; Laezza, F. Identification of Amino Acid Residues in Fibroblast Growth Factor 14 (FGF14) Required for Structure-Function Interactions with Voltage-Gated Sodium Channel $Na_v1.6$. *J. Biol. Chem.* **2016**, *291*, 11268–11284. [CrossRef] [PubMed]
26. Ali, S.R.; Liu, Z.; Nenov, M.N.; Folorunso, O.; Singh, A.; Scala, F.; Chen, H.; James, T.F.; Alshammari, M.; Panova-Elektronova, N.I.; et al. Functional Modulation of Voltage-Gated Sodium Channels by a FGF14-Based Peptidomimetic. *ACS Chem. Neurosci.* **2018**, *9*, 976–987. [CrossRef]
27. Singh, A.K.; Wadsworth, P.A.; Tapia, C.M.; Aceto, G.; Ali, S.R.; Chen, H.; D'Ascenzo, M.; Zhou, J.; Laezza, F. Mapping of the FGF14:$Na_v1.6$ Complex Interface Reveals FLPK as a Functionally Active Peptide Modulating Excitability. *Physiol. Rep.* **2020**, *8*, e14505. [CrossRef]
28. Singh, A.K.; Dvorak, N.M.; Tapia, C.M.; Mosebarger, A.; Ali, S.R.; Bullock, Z.; Chen, H.; Zhou, J.; Laezza, F. Differential Modulation of the Voltage-Gated Na+ Channel 1.6 by Peptides Derived From Fibroblast Growth Factor 14. *Front. Mol. Biosci.* **2021**, *8*, 860. [CrossRef] [PubMed]
29. James, T.F.; Nenov, M.N.; Wildburger, N.C.; Lichti, C.F.; Luisi, J.; Vergara, F.; Panova-Electronova, N.I.; Nilsson, C.L.; Rudra, J.S.; Green, T.A.; et al. The $Na_v1.2$ Channel Is Regulated by GSK3. *Biochim. Biophys. Acta (BBA)-Gen. Subj.* **2015**, *1850*, 832–844. [CrossRef] [PubMed]
30. Wang, P.; Wadsworth, P.A.; Dvorak, N.M.; Singh, A.K.; Chen, H.; Liu, Z.; Zhou, R.; Holthauzen, L.M.F.; Zhou, J.; Laezza, F. Design, Synthesis, and Pharmacological Evaluation of Analogues Derived from the PLEV Tetrapeptide as Protein–Protein Interaction Modulators of Voltage-Gated Sodium Channel 1.6. *J. Med. Chem.* **2020**, *63*, 11522–11547. [CrossRef]

31. Dvorak, N.M.; Wadsworth, P.A.; Wang, P.; Chen, H.; Zhou, J.; Laezza, F. Bidirectional Modulation of the Voltage-Gated Sodium ($Na_v1.6$) Channel by Rationally Designed Peptidomimetics. *Molecules* **2020**, *25*, 3365. [CrossRef]
32. Dong, X.-W.; Priestley, T. Electrophysiological Analysis of Tetrodotoxin-Resistant Sodium Channel Pharmacology. *Curr. Protoc. Pharmacol.* **2004**, *23*, 11.8.1–11.8.33. [CrossRef]
33. Tapia, C.M.; Folorunso, O.; Singh, A.K.; McDonough, K.; Laezza, F. Effects of Deltamethrin Acute Exposure on $Na_v1.6$ Channels and Medium Spiny Neurons of the Nucleus Accumbens. *Toxicology* **2020**, *440*, 152488. [CrossRef]
34. Palmer, B.D.; Thompson, A.M.; Booth, R.J.; Dobrusin, E.M.; Kraker, A.J.; Lee, H.H.; Lunney, E.A.; Mitchell, L.H.; Ortwine, D.F.; Smaill, J.B.; et al. 4-Phenylpyrrolo[3,4-c]Carbazole-1,3(2H,6H)-Dione Inhibitors of the Checkpoint Kinase Wee1. Structure−Activity Relationships for Chromophore Modification and Phenyl Ring Substitution. *J. Med. Chem.* **2006**, *49*, 4896–4911. [CrossRef] [PubMed]
35. Goldfarb, M.; Schoorlemmer, J.; Williams, A.; Diwakar, S.; Wang, Q.; Huang, X.; Giza, J.; Tchetchik, D.; Kelley, K.; Vega, A.; et al. Fibroblast Growth Factor Homologous Factors Control Neuronal Excitability through Modulation of Voltage-Gated Sodium Channels. *Neuron* **2007**, *55*, 449–463. [CrossRef] [PubMed]
36. Wang, C.; Wang, C.; Hoch, E.G.; Pitt, G.S. Identification of Novel Interaction Sites That Determine Specificity between Fibroblast Growth Factor Homologous Factors and Voltage-Gated Sodium Channels. *J. Biol. Chem.* **2011**, *286*, 24253–24263. [CrossRef]
37. Laezza, F.; Gerber, B.R.; Lou, J.-Y.; Kozel, M.A.; Hartman, H.; Craig, A.M.; Ornitz, D.M.; Nerbonne, J.M. The FGF14(F145S) Mutation Disrupts the Interaction of FGF14 with Voltage-Gated Na^+ Channels and Impairs Neuronal Excitability. *J. Neurosci.* **2007**, *27*, 12033–12044. [CrossRef] [PubMed]
38. Di Re, J.; Wadsworth, P.A.; Laezza, F. Intracellular Fibroblast Growth Factor 14: Emerging Risk Factor for Brain Disorders. *Front. Cell. Neurosci.* **2017**, *11*, 103. [CrossRef]
39. Wildburger, N.C.; Ali, S.R.; Hsu, W.-C.J.; Shavkunov, A.S.; Nenov, M.N.; Lichti, C.F.; LeDuc, R.D.; Mostovenko, E.; Panova-Elektronova, N.I.; Emmett, M.R.; et al. Quantitative Proteomics Reveals Protein-Protein Interactions with Fibroblast Growth Factor 12 as a Component of the Voltage-Gated Sodium Channel 1.2 ($Na_v1.2$) Macromolecular Complex in Mammalian Brain. *Mol. Cell. Proteom.* **2015**, *14*, 1288–1300. [CrossRef]
40. Dover, K.; Solinas, S.; D'Angelo, E.; Goldfarb, M. Long-Term Inactivation Particle for Voltage-Gated Sodium Channels. *J. Physiol.* **2010**, *588*, 3695–3711. [CrossRef] [PubMed]
41. Liu, C.J.; Dib-Hajj, S.D.; Waxman, S.G. Fibroblast Growth Factor Homologous Factor 1B Binds to the C Terminus of the Tetrodotoxin-Resistant Sodium Channel $RNa_v1.9a$ (NaN). *J. Biol. Chem.* **2001**, *276*, 18925–18933. [CrossRef]
42. Hennessey, J.A.; Marcou, C.A.; Wang, C.; Wei, E.Q.; Wang, C.; Tester, D.J.; Torchio, M.; Dagradi, F.; Crotti, L.; Schwartz, P.J.; et al. FGF12 Is a Candidate Brugada Syndrome Locus. *Heart Rhythm* **2013**, *10*, 1886–1894. [CrossRef]
43. Yang, L.; Dong, F.; Yang, Q.; Yang, P.-F.; Wu, R.; Wu, Q.-F.; Wu, D.; Li, C.-L.; Zhong, Y.-Q.; Lu, Y.-J.; et al. FGF13 Selectively Regulates Heat Nociception by Interacting with $Na(_v)1.7$. *Neuron* **2017**, *93*, 806–821.e9. [CrossRef] [PubMed]
44. Wang, Q.; Yang, J.; Wang, H.; Shan, B.; Yin, C.; Yu, H.; Zhang, X.; Dong, Z.; Yu, Y.; Zhao, R.; et al. Fibroblast Growth Factor 13 Stabilizes Microtubules to Promote Na+ Channel Function in Nociceptive DRG Neurons and Modulates Inflammatory Pain. *J. Adv. Res.* **2021**, *31*, 97–111. [CrossRef]
45. Hsu, W.-C.J.; Scala, F.; Nenov, M.N.; Wildburger, N.C.; Elferink, H.; Singh, A.K.; Chesson, C.B.; Buzhdygan, T.; Sohail, M.; Shavkunov, A.S.; et al. CK2 Activity Is Required for the Interaction of FGF14 with Voltage-Gated Sodium Channels and Neuronal Excitability. *FASEB J.* **2016**, *30*, 2171–2186. [CrossRef] [PubMed]
46. Spratt, P.W.E.; Alexander, R.P.D.; Ben-Shalom, R.; Sahagun, A.; Kyoung, H.; Keeshen, C.M.; Sanders, S.J.; Bender, K.J. Paradoxical Hyperexcitability from $Na_V1.2$ Sodium Channel Loss in Neocortical Pyramidal Cells. *Cell Rep.* **2021**, *36*, 109483. [CrossRef] [PubMed]
47. Hu, W.; Tian, C.; Li, T.; Yang, M.; Hou, H.; Shu, Y. Distinct Contributions of Na(v)1.6 and Na(v)1.2 in Action Potential Initiation and Backpropagation. *Nat. Neurosci.* **2009**, *12*, 996–1002. [CrossRef]
48. Osorio, N.; Cathala, L.; Meisler, M.H.; Crest, M.; Magistretti, J.; Delmas, P. Persistent $Na_v1.6$ Current at Axon Initial Segments Tunes Spike Timing of Cerebellar Granule Cells. *J. Physiol.* **2010**, *588*, 651–670. [CrossRef]
49. Royeck, M.; Horstmann, M.-T.; Remy, S.; Reitze, M.; Yaari, Y.; Beck, H. Role of Axonal $Na_V1.6$ Sodium Channels in Action Potential Initiation of CA1 Pyramidal Neurons. *J. Neurophysiol.* **2008**, *100*, 2361–2380. [CrossRef]